PERGAMON

Nonlinear Analysis 47 (2001) 245–256

Nonlinear Analysis

www.elsevier.nl/locate/na

Individual-based models to growth and folding in one-layered tissues: Intestinal crypts and early development

Dirk Drasdo and Markus Loeffler

Inst. for Medical Informatics, Statistics and Epidemiology
University of Leipzig
Liebigstr. 27
D-04103 Leipzig, Germany

Abstract

In this paper we present individual-based models of the spatio-temporal dynamics in one-layered multicellular biological systems and outline how they can be adapted to experimental systems (individuum here: single cell). Mathematically these systems present a new and interesting class of problems which allow to study how to link individual-based models with continuum theory in problems with internally growing manifolds.

As model systems we mainly focus on intestinal crypts since they are paradigmatic in several regards: (i) they represent a simple epithelial tissue, (ii) they contain only a small number of cells ($N \approx 300$), (iii) much is known about them and they are fairly well accessible to experiments, (iv) perturbations in their spatio-temporal dynamics have been found to result in folded patterns (crypt fission, polyps and adenoma) which are pre-patterns of intestinal cancer.

We show how the formation of folded patterns can be explained within a single-cell based, lattice-free model. We further illustrate, that the folding principles are expected to carry over to other tissue layers as well as to a developing blastula or the oral mucosa supported by computer simulations and a simple field theory.

Key words: Individual-based modeling, continuum model, one-layered tissues, intestinal crypt, blastulation, buckling
PACS:

1 Introduction

The understanding of the principles underlying the complicated spatial-temporal processes during morphogenesis and tissue maintenence require a model or a

PII: S0362-546X(01)00173-0

class of models capable to consider adequately the many degrees of freedom specific to multicellular systems. An essential difference to physical or chemical multi-particle systems is the particular ability of each individual biological cell to change its physical properties by differentiation, i.e. a program determined on the time scale of evolution. Differentiation leads to different cell types in multicellular assemblies on length scales of several cell diameters. These requirements favor single cell based models as a general framework. However, many models that differ in a number of details show a similar structural or generic behavior which allows to extract a number of classes much smaller than those possible by the number of parameters and their possible range or the degrees of freedom. Unfortunately, single-cell based computer simulations alone are often not capable to identify generic behavior since (i) generic regimes often show up only on large time or length scales not accessible to a computer simulation, (ii) it often cannot be ruled out that for parameter combinations different from those used in the computer simulations the observed behavior may change.
A potential strategy to deal with this problem is to search for simple generic equations that include the relevant physics of the problem and extract the generic behavior from them. The generic behavior then should be insensitive to changes of parameters or details in the setup of the model and may even be found in completely different situations.

In this paper we present single-cell lattice-free models for the normal and perturbed dynamics in intestinal crypts and blastula formation in sea urgin or synapta digita. Crypts are the cell proliferating units in the intestine, blastula formation is the first step in early embryonic development after a zygote has developed. These systems are examples of one-layered tissues and the models base on the same approach. The results of computer simulations with these models suggest that folding in one-layered tissues, as observed e.g. in crypt fission [1] - [4], results from a buckling instability of the Euler type [5], [6]. The model further predicts conditions under which we expect the same type of dynamical instability in blastula formation [7]. The principles of the folding mechanism are explained within a simple coarse gained analytical approach.

2 Crypt fission

Crypts form pear-shaped, one cell thick pockets in the intestinal wall surrounded by connective tissue [8]. Between the crypts muscle cells can be found that enclose the intestinal mucosa and may contribute to the stability of the crypt shape. The orifice of the crypts is fixed in the intestinal mucosa and oriented toward the intestinal lumen. Hence the crypt lumen is connected with the intestinal lumen. Crypts have $N =\sim 300$ cells in total, ~ 15 cells in perimeter and ~ 20 cells from the closed bottom to the orifice. The cell size is

$l =\sim 6 - 10\mu m$. Crypts are responsible for the maintenence of the high-cell turnover in the intestine. After $T =\sim 1 - 2d$ a crypt has completely renewed all its cells. Most of the cell divisions take place in the lower 2/3 of the crypts. The typical cell cycle time is $\tau =\sim 12h$. The newly generated cells then migrate toward the orifice of the crypt. From there (or from the tip of the "villi", inward pointing one-cell thick cones; this depends on the species under consideration) they are released into the intestinal lumen. The one-cell thick crypt epithelium is made up of polar cells. Their apical membrane points toward the crypt lumen. They bind to their neighbor cells by adhesive contacts in their side membranes and are attached to an extracellular basal membrane. Below the basal membrane is connective and muscle tissue.

After x-ray irradiation of 10Gy or more cell division stops for a short period of time followed by a period of very rapid cell division where either the crypt cell layer folds or the crypt completely disappears [1], [2]. Similar folded patterns are observed during the formation of polyps and adenoma which form prepatterns of intestinal cancer [3], [4]. In hereditary forms of intestinal cancer, gene defects have been identified in cancer cells that encode proteins responsible for the stability of the cell-cell contacts (e.g. [9]). The exact mechanisms responsible for the folded pattern are mainly unknown in all these cases. In particular is yet not clear if the folded pattern after x-ray irradiation and in crypt cancer formation have the same mechanistic origin. In the following we present a model that we hope contributes to answer this question.
In the past 15 years a number of spatial models have been established in order to explain different aspects of the cell kinetics in individual intestinal crypts. Most models are based on cellular automata and use division and migration rules (e.g. [10] – [15]). None of these models allows for shape changes hence they are not suited to study how the crypt shape may be stabilized or destabilized during fission. In this paper we discuss, for the first time, a model that is capable to cover shape changes of crypts.

For simplicity we here consider a 2d vertical section through a crypt. Hence we consider the simpler case of a cell chain instead of cell sheet. (As we will argue below we believe that this does not affect the relevant physics.) We approximate a cell in the interphase of the cell cycle by a circle (figure 1a). In the beginning of the interphase the cell radius is minimal and increases until the cell area (= mass) has doubled at the end of the interphase. The interphase is followed by mitosis where the cell deforms into a dumb-bell at constant area. We assume that only cells for which $y < y^t - y^b + 3x^s$ hold are able to reenter the division cycle after having finished their last division (for def. of y, y^t, x^s, see figure 1b). In this case the lower $\sim 2/3$ of a crypt of normal length are populated by dividing cells, as experimentally observed. This further is compatible with the results of two competing concepts to explain the cell kinetics in the crypt: (i) the "pedigree concept" which assumes that a few stem cells at the crypt bottom ($\sim 4 - 8$) produce a number of "transient cells"

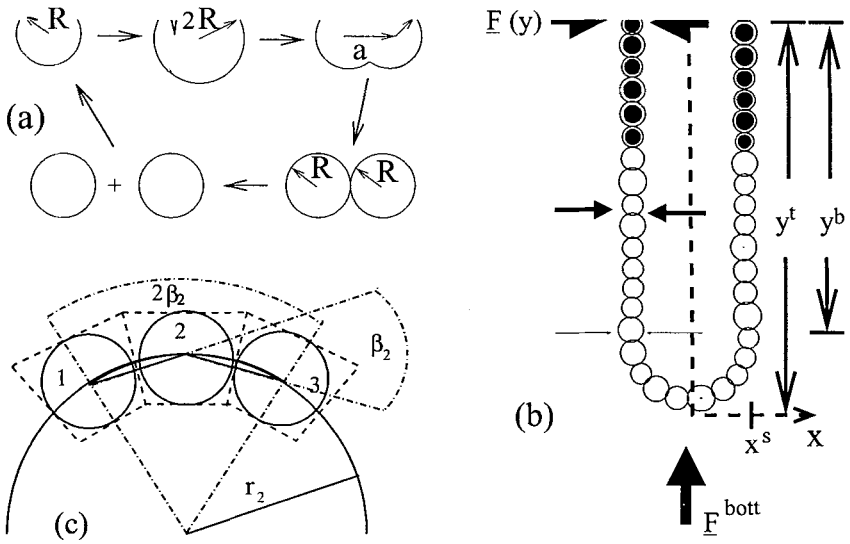

Fig. 1. (a) Cell division algorithm in the computer simulation. During the interphase the cell increases its radius from $R \to \sqrt{2}R$ in small steps ξ, where ξ is a uniformly distributed random number in the interval $0 \leq \xi \leq \xi^{max}$ with $\xi^{max} \ll R$. During mitosis the cell deforms into a dumb-bell and divides as far as the mother cell has the same shape as the collective envelope of the two neighboring daughter cells. (b) Sketch of a 2d-section through a single crypt. The 3d-shape is obtained by rotating the 2d-crypt around the y-axis. The filled circles mark cells that cannot perform a further cell division. For the left branch of the crypt arrows are drawn indicating the direction and strength of the force exerted by surrounding tissue and due to the stabilizing effect of shear forces (see text). Larger arrows indicate larger forces. (c) Bent cell configuration. The angle β_2 and the radius of curvature, r_2 characterize the local curvature at the position of cell 2. The trapezoids indicate the position of the cell membranes, the circles the abstraction used in the computer simulations. The parameters in the model equations can be related to geometric and elastic constants by comparing a cell configuration with a bent bar.

which are capable of only a limited number ($\sim$ 3) of further cell divisions and then change into "mature cells" that cannot divide anymore [16], (ii) a morphogene concept, in which only cells with a local morphogene concentration larger than a certain threshold are able to enter the cell cycle [14]. The morphogene is released from the bottom of the crypts. In order to ensure a one-cell thick structure is maintained any cell i attempt to orientate its axis along the tangent to the local radius of curvature r_i (which we denote as the optimal orientation, see figure 1c). For cell movements (orientational changes or displacements) we assume that friction terms are large compared to inertia terms since extracellular components provide a strong friction-like resistance to cell movements [17], [18], [19]. Further, experiments suggest, that stochastic components in cell movement can be neglected [20]. For orientational changes of a cell i this results in

$$\frac{d\alpha_i}{dt} = -\tilde{\eta}(\alpha_i - \alpha_i^{(0)}). \tag{1}$$

where the angle α_i describes the momentary, $\alpha_i^{(0)}$ the optimal orientation of the cell axis. $\tilde{\eta}$ subsumes the torque actively exerted from the cell on its environment and the viscosity of the cell environment. We assume $\tilde{\eta} \gg 1$.
The equation for the displacement of a cell i reads:

$$\gamma \frac{d\underline{r}_i}{dt} = \underline{F}_i \tag{2}$$

where γ is the friction constant and $\underline{F}_i$ is the total force on a single cell given by

$$\underline{F}_i = \underline{F}_i^{NN} + \underline{F}_i^{bend} + \underline{F}_i^{bott} + \underline{F}^s(y). \tag{3}$$

The friction constant γ can be estimated from a "cellular Einstein relation"

$$\gamma = D/F_T, \tag{4}$$

and $D = 4.6\ 10^{-16} m^2/s$, $F_T \approx 10^{-15} J$ measured by Beysens, Forgacs and Glazier [21] for embryonic chicken cells. The corresponding parameters specific to crypts are not known. In order to obtain a dynamically stable crypt we had to assume a 10-times larger viscosity γ (e.g. by choosing $F_T = 10^{-16} J$ and keeping the value for D constant).

Figure 1c shows a sketch which illustrates the forces acting on the crypt cells from connective or muscle tissue.

The forces are defined as follows:

$$\underline{F}_i^{NN} = \sum_{j\ NN\ i} \underline{F}_{ij}^{NN} = -k_{NN} \sum_{j\ NN\ i} \left(d_{ij} - d_{ij}^{(0)}\right) \frac{\underline{r}_j - \underline{r}_i}{d_{ij}} \tag{5}$$

denotes the elastic forces between two cells connected by adhesive bonds. d_{ij} is the distance between the centers of two neighboring cells, $d_{ij}^{(0)}$ their equilibrium distance.
Since the cells are polar, a sheet of cells may be considered similar to a membrane and hence is stabilized by a bending force [6], [7], [22]:

$$\underline{F}_i^{bend} = \sum_{j=i}^{i+2} -\frac{dv_{\beta_j}(\beta_j)}{dcos(\beta_j)} \frac{dcos(\beta_j)}{d\underline{r}_i} \tag{6}$$

where

$$v_\beta(\beta_j) = \frac{k_b}{2}\left(\beta_j - \beta_j^{(0)}\right)^2 \tag{7}$$

β_j characterizes the curvature of the cell chain at the position of cell j (figure 1c), $\beta_j^{(0)}$ the spontaneous curvature. $\beta_j^{(0)} = 0$ ($\beta_j^{(0)} \neq 0$) results if each cell in a given configuration tries to adopt the shape of a perfect rectangle (trapezoid). $k_b = \kappa/l$ where κ is the bending rigidity and l the cell diameter. The force from the tissue below the crypt is assumed to act only on cells in the semi-spherical bottom and is assumed as

$$\underline{F}_i^{bott} = -k_{bott}(y_i - y_i^t)\underline{e}_y \tag{8}$$

y_i^t is the crypt height (see figure 1), k_{bott} the corresponding spring constant and $\underline{e}_y$ the unit vector in positive y-direction.

There is a number of additional forces stabilizing the crypt shape:
(i) shear forces, because displacements perpendicular to the crypt walls increases the shear energy in the cylindrical shaped part of the crypt. Shear forces are a feature of $d > 1$-dimensional non-fluid manifolds. Their effect can only be considered by a crude approximation in 1d-cell chains.
(ii) a force from the connective tissue around the crypt.
(iii) The crypt orifice is anchored in the epithelium of the intestinal lumen which stabilizes the orifice. This force declines towards the crypt bottom.
We summarize these forces in a very simple heuristic ansatz by

$$\underline{F}_i^s \approx \begin{cases} -k_s(y)(x - x^s)\underline{e}_x \; for \; x > 0 \wedge y \geq (y^t - y^b) \\ -k_s(y)(x + x^s)\underline{e}_x \; for \; x < 0 \wedge y \geq (y^t - y^b) \end{cases} \tag{9}$$

with $k_s(y) \approx k_{side}\frac{k_{NN}}{y^t - y^b}y - \frac{k_{NN}y^b}{y^t - y^b}$. x and x^s are defined in Figure 1b.
The constants k_{NN} and k_b can be expressed in terms of the Young modulus and parameters characterizing the geometry of the cell and the basal layer [7]. The Young moduli in crypts have not yet been determined. We have chosen the Young moduli for the cells and the basal membrane to $E = 400Pa$ and $E = 4400Pa$ according to estimates from Davidson et.al. for sea urgin [23]. The constants k_{bott}, k_{side} are adjusted in such a way, that (i) the crypt approximately maintains a length of $y_b/l \approx 20 - 24$. (ii) the dynamics reproduces the correct crypt turnover time T.

We performed simulations with different seeds of the random generator and broke up the simulations after times that correspond to the life span of mice. We found the crypts remained stable and maintained their average length and turnover time over the simulation time.

Radiation as well as mutations found in polyps, adenoma and cancer indicate

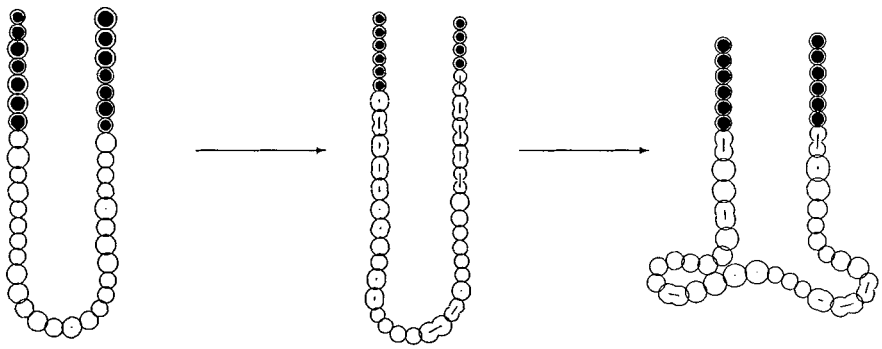

Fig. 2. Typical fission scenario in a crypt. From $t/\tau = 0$ (i) to $t/\tau = 5$ (ii) the crypt is stable. At (ii) we changed $\kappa \to \kappa/5$. This destabilizes the crypt and results in fission (iii).

a perturbed cell kinetics, the anatomic changes of the folded crypt a perturbed crypt mechanics. However, neither the genetic mechanisms nor the cooperative cell behavior responsible for the observed folded pattern are yet well understood. In particular it is unclear if and how genetic mutations effect the cell kinetics or the material parameters. The experimental observations reported in the beginning of this section suggest both modes of action, a reduction in the mechanical stability of the crypt cell layer and changes in the cell cycle time. We model these effects (i) by reducing the Young modulus of the cells, which results in a reduction of k_b and k_{NN} and (ii) by changing the cell cycle time. In both cases, instabilities are observed that look similar to those in the experiment. Fig. 3 shows an example for $k_b \to k_b/5$ and $k_{NN} \to k_{NN}/5$, where an instability in the crypt bottom occurs.

The simulation results suggest that the generation of arclength (by cell divisions) cannot be balanced anymore by a sufficiently fast cell migration toward the crypt orifice (where the arclength is extinguished) if the bending rigidity becomes too small or the cell cycle time too large. The newly generated arclength cannot fully be absorbed into a smooth layer but evades perpendicular to the cell layer. This becomes visible macroscopically as buckling.

3 Early embryonic development: blastula formation

During blastula formation in sea urgin or synapta digita a hollow, one-cell thick sphere is formed by successive, cell division from the zygote [24]. The number

of cells increases exponentially. After each cell division the two daughter cells have half of the mass of their mother cell such that the total embryo mass does not increase ("cleavage", figure 3). As in the crypt cleavage is directed in

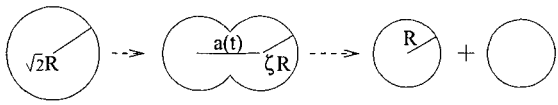

Fig. 3. Cleavage in the computer simulation. The cell deforms by decreasing its instantaneous radius in small steps, i.e. $\tilde{R}(t) = \zeta(t)R$ $(\zeta(t) \geq 1)$ from R (at $t = 0$) $\to R/\sqrt{2}^m$(at $m = t/\tau$). m is the number of divisions the cell has performed from $t = 0$ (zygote stage) until t. The quantity $\zeta(t)$ contains information on the cumulative effect of these small steps. Accordingly, the axis $a(t)$ increases to keep the total area of the cell constant during one division cycle.

such a way that the single-cell thick structure is maintained. I.e., once a hollow sphere is formed the cleavage direction is always tangential to the surface. At a size of $N \approx 1000$ cells, cleavage stops and an invagination in a small circular area of the hollow sphere occurs ("gastrulation"). From the invaginated part, the digestive tract is formed during further development.

As in the case of intestinal crypts we assume that the one-cell thick structure is maintained by polar cells that perform directed cleavage [7]. Again we assume a first-order dynamics. Since different from crypt cells the cells during blastula formation experience only very small displacements the effect of noise cannot be neglected [7]. Such a dynamics can be described by the Metropolis algorithm and corresponds to the numerical integration of a corresponding master equation [6], [17]. The application of the Metropolis algorithm requires the calculation of the total configuration energy V^{tot}. A cell movement (displacement or rotation) occurs with probability one if it decreases the total configuration energy ($\Delta V^{tot} < 0$) and with probability $1 - \exp(-\Delta V^{tot}/F_T)$ if $\Delta V^{tot} \geq 0$. We here consider only contributions from nearest-neighbor-interactions, bending and a rotational energy. We use the same elastic constants as above for the cells and the layer enclosing the cell layer (the "hyaline layer") (for details see [7]). The size of the zygote is $l =\sim 50\mu m$, the cycle time $\tau =\sim 1h$.

Starting with a single cell, after a number of successive cell divisions a hollow blastula emerges. If cleavage proceeds beyond the size of a blastula at the onset of gastrulation, a buckling instability occurs (figure 4). This may be verified experimentally if gastrulation is suppressed and blastula formation proceeds.

The underlying folding mechanism can best be understood from a simple continuum approach [6]. Connecting the centers of the cells in a circular configuration we arrive at a closed 1d-manifold in 2d which can be characterized by the position vector $\underline{r}(\alpha, t)$. Here $\alpha \in [0, 1)$ is a parameter, t the time. $\underline{r}(\alpha, t)$ and its first two derivatives with respect to α are periodic in α. The (overdamped)

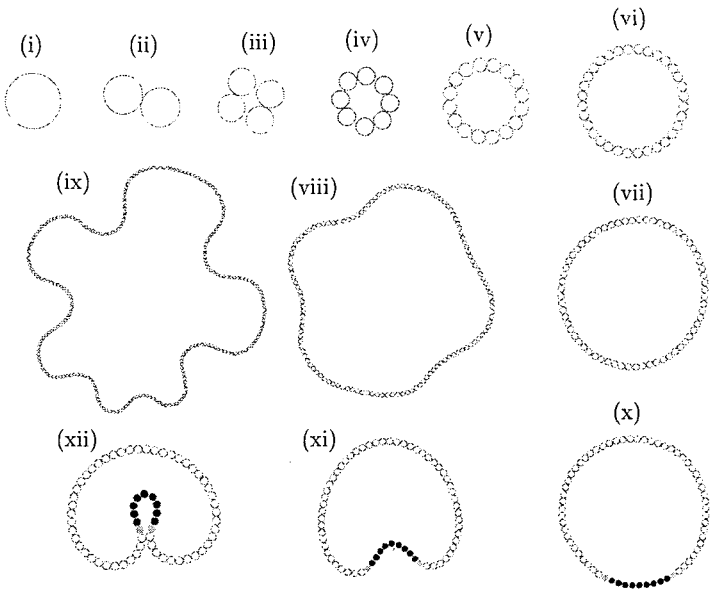

Fig. 4. Typical simulation run for blastula formation (i)-(vi) and gastrulation (vii),(x)-(xii). Pictures (viii) and (ix) show a buckling instability, expected if gastrulation would not happen but cleavage would go on. The dark cells in (x)-(xii) have a negative spontaneous curvature c_s, i.e., their preferred state is a trapezoid-shape with the shorter side pointing outward, the larger side pointing inward. This takes into account an active cell change in a limited area of the blastula at the end of blastulation yields an invagination after a differentiation has occurred [7], [25].

dynamics then can be described by the field equations

$$\zeta \left.\frac{\partial \underline{r}(\alpha,t)}{\partial t}\right|_{\alpha} = -\frac{1}{\sqrt{g}}\frac{\delta \Phi}{\delta \underline{r}}, \tag{10}$$

$$\partial_t \sqrt{g} = \sigma \sqrt{g}. \tag{11}$$

Here, ζ is the friction density, $g = \partial_\alpha \underline{r}(\alpha,t)\partial_\alpha \underline{r}(\alpha,t)$ the determinant of the metric tensor. $\Phi = \Phi_0(\alpha,t) - \int_0^1 \Lambda(\alpha,t)\sqrt{g}d\alpha$, where $\Lambda(\alpha,t)$ is a Lagrangian multiplier field which couples the condition to the time evolution of the local metric (eqn. (11)) to the equation of motion for $\underline{r}(\alpha,t)$ (eqn. (10)). $\Phi_0 = (\kappa/2)\int_0^1 (c(\alpha,t) - c_s)^2\sqrt{g}d\alpha$ is the bending energy, κ the bending rigidity. $c(\alpha,t)$ is the local, c_s the spontaneous curvature. σ is the growth rate. The choice of the r.h.s. of eqn. (11) ensures exponential growth as found in the computer simulation and experimentally. A linear stability analysis around the homogeneous state, a perfect circle, shows that a buckling instability must occur at sufficiently large circle radii. The existence of the instability is hence neither a feature or artefact of the computer model nor depend on particular

details in the setup of the model. If κ is reduced or the growth rate σ increased, the instability occurs at smaller radii.

4 Discussion

In this paper we discussed two examples of dynamic form formation and maintenence in one-layered growing tissues. Both examples, the maintenence and folding of intestinal crypts and the formation of a blastula, base on a single cell approach. In each case we assumed an overdamped dynamics for cell migration and rotation, in crypts in the limit of vanishing noise and in the blastula where noise cannot be neglected. The driving force for cell displacement is cell division. We assumed the bending energy provides a major contribution to stabilize a one-cell thick epithelium, similar to the situation in membranes [26], [27]. In computer simulations we found the same type of buckling instability in both systems. The mechanism underlying this instability was explained within a simple continuum approach. It suggests a layer roughens and folds if the bending energy isn't sufficiently large to smoothen stochastic fluctuations perpendicular to the cell layer. This occurs the easier, the smaller is the bending rigidity and the larger is the growth rate. A small bending rigidity reduces the resistance against bending of a cell layer, an increase of the growth rate reduces the time to relax existent transversal fluctuations of a cell layer. The mechanism is believed to be generic and to hold also in three dimensions although in 3d shear stress may elevate the energy barrier for the instability. Note in this context that cell assemblies can behave as a viscoelastic fluid and are often able to reorganize in order to reduce shear energy contributions on large time scales [28].
We believe that the folding principle does not only hold for single-layered structures but also for multi-layered structures if cell proliferation in the complete or a sub-layer is not balanced by a sufficiently fast migration of cells out of this layer. A situation that supports this line of argument can be found in the oral mucosa, the skin of the mouth. After administration of a growth factor that increases cell division prominent buckling of the basal membrane, the lowest and strongest proliferating cell layer, is observed [29].

Acknowledgment

We thank C. Booth, F. Meineke and C.S. Potten for helpful discussions about intestinal crypts. DD. gratefully acknowledges the contribution of G. Forgacs to blastulation. This work was supported by the Deutsche Forschungsgemeinschaft under Grant No. Lo 345/4-3.

References

[1] Cairnic, A.B. and Millen, B.H., Fission of Crypts in the small Intestine of the irradiated mouse, *Cell Tissue Kinet.* **8** 89 - 196 (1975).

[2] Booth, C. and Potten, C.F., Gut instincts, thoughts on intestinal epithelial stem cells, *J. Clin. Invest.* **105** (11) 1493 - 1499 (2000).

[3] Araki, K., Ogata, T., Kobayashi, M. and Yatani, R., A Morphological Study on the Histogenesis of Human Colorectal Hyperplastic Crypts, *Gastroenterology* **109** 1468-1474 (1995).

[4] Wright, N.A., Epithelial stem cell repertoire in the gut: clues to the origin of cell lineages, proliferative units and cancer, *Int. J. Exp. Path.* **81**, 117-143 (2000).

[5] Moldovan, D. and Golubovic, L., Buckling Dynamics of Compressed Thin Sheets (Membranes) *Phys. Rev. Lett.* **81** 2884-2887 (1999).

[6] Drasdo, D. Buckling Instabilities in One-Layered Growing Tissues. *Phys. Rev. Lett.* **84** 4424 - 4427 (2000).

[7] Drasdo, D. and Forgacs, G., Modeling generic and genetic interactions in Cleavage, Blastulation and Gastrulation. *Dev. Dyn.* **219** (2) (2000).

[8] Wright, N. and Alison, N. The biology of epithelial cell populations. Oxford, Clarendon Press. Vol. I,II (1984).

[9] Huelsken, J., Behrens, J. and Birchmeier, W., Tumor-suppressor gene products in cell contacts: the cadherin-APC-armadillo connection, *Curr. Op. Cell Biol.* **6**, 711-716 (1994).

[10] Loeffler, M., Stein, R., Wichmann, H.E., Potten, C.S., Kraur., P., Chwalinski, S., Intestinal cell proliferation I. A comprehensive model of steady-state proliferation in the crypt. *Cell Tissue Kinet.* **19**, 627 - 645 (1986).

[11] Finney, K.J., Appleton, D.R., Ince, P., Sunter, J.P., Watson, A.J., Proliferative status of colonic mucosa in organ culture: 3H-thymidine-labeling studies and computer modeling. *Virchows Arch. B Cell Pathol. Incl. Mol. Pathol* **56**, 397-405 (1989).

[12] Meinzer, H.P., Sandblad, B., Baur, H.J., Generation-dependent control mechanisms in cell proliferation and differentiation-the power of two. *Cell Prolif.* **25**, 125-40 (1992).

[13] Paulus, U., Loeffler, M., Zeidler, J., Owen, G. and Potten, C.S., The differentiation and lineage development of goblet cells in the murine and small intestinal crypt: experimental and modeling studies, *J. Cell Sci.* (104), 473 - 484 (1993).

[14] Gerike T.G., Paulus U., Potten C.S., Loeffler M., A dynamic model of proliferation and differentiation in the intestinal crypt based on a hypothetical intraepithelial growth factor, *Cell Prolif.* **31** (2) 93-110 (1998).

[15] Isele, W.P., Meinzer, H.P., Applying computer modeling to examine complex dynamics and pattern formation of tissue growth. *Comput. Biomed. Res.* **31**, 476-94 (1998).

[16] Potten, C.S., Loeffler, M., Stem cells: attributes, cycles, spirals, pitfalls and uncertainties. Lessons for and from the crypt, *Development* **110** 1001 - 1020 (1990).

[17] Drasdo, D., Kree, R. and McCaskill, J.S., A Monte Carlo Model to tissue cell populations, *Phys. Rev. E* **52** (6) 6635-6657 (1995).

[18] Drasdo, D., Different growth regimes found in a Monte-Carlo Model of growing tissue cell populations, pp. 281 - 291, in F. Schweitzer (ed.): Self organization of complex structures: From individual to collective dynamics. Gordon and Breach (1996).

[19] Meineke, F.A., Potten, S.C. and Loeffler, M., Cell migration and organization in the intestinal crypt using a lattice-free model, subm. to *Cell Proliferation.*

[20] Potten, C.S., Booth, C., Pritchard, D.M., The intestinal epithelial stem cell: the mucosal governor. *Int. J. Exp. Pathol.* **78** 219 - 43. (1997).

[21] Beysens, D., Forgacs, G. and Glazier, J.A.: Cell sorting is analogous to phase ordering in fluids, *PNAS* **97** (17) 9467 - 9471 (2000)

[22] Allen, M.P., Tildesley, D.J., Computer Simulation of Liquids, Oxford Science Publ. (1987).

[23] Davidson, L.A., Koehl, M.A.R., Keller, R. and Oster, G.F. How do sea urchins invaginate? Using bio-mechanics to distinguish between mechanisms of primary invagination. *Development*, **121** 2005-2018 (1995).

[24] Gilbert, S.F. Developmental Biology. Sinauer Associates, Sunderland (1997).

[25] Kam, Z., Minden, J., Agard, D., Sedat, J.W. and Leptin, M. Drosophila gastrulation: analysis of cell shape changes in living embryos by three-dimensional fluorescence microscopy. *Development* **112** 365 - 370 (1991).

[26] Svetina, S. and Zeks, B., Mechanical behavior of closed lamellar membranes as a possible common mechanism for the establishment of developmental shapes, *Int. J. Dev. Biol.* **35**, 359 - 365 (1991).

[27] Seifert, U., Configurations of fluid membranes and vesicles, *Advances in Physics*, **46** (1), 13 - 137 (1997).

[28] Forgacs, G., Foty, R.A., Shafrir, Y., Steinberg, M.S. Viscoelastic Properties of living embryonic tissues - A Quantitative Study, *Biophys. J.* **74** (5) 2227 - 2234 (1998).

[29] Farrell, C.L., Rex, K.L., Kaufman, S.A., Dipalma, C.R., Chen, J.N., Scully, S. and Layey, D.L., Effects of keratinocyte growth factor in the squamous epithelium of the upper aero-digestive tract of normal and irradiated mice, *Int. J. Radiat. Biol.* **75** (5) 609-620 (1999).